cancers

MDPI

Article

Significance of LIF/LIFR Signaling in the Progression of Obesity-Driven Triple-Negative Breast Cancer

Lois Randolph [1], Jaitri Joshi [2], Alondra Lee Rodriguez Sanchez [1], Uday P. Pratap [1], Rahul Gopalam [1], Yidong Chen [3,4], Zhao Lai [3,5], Bindu Santhamma [6], Edward R. Kost [1], Hareesh B. Nair [6], Ratna K. Vadlamudi [1,7,8], Panneerdoss Subbarayalu [3,*] and Suryavathi Viswanadhapalli [1,7,*]

1 Department of Obstetrics and Gynecology, University of Texas Health San Antonio, San Antonio, TX 78229, USA; randolphl@uthscsa.edu (L.R.); rodriguezsaa@uthscsa.edu (A.L.R.S.); pratap@uthscsa.edu (U.P.P.); gopalam.rahul@gmail.com (R.G.); kost@uthscsa.edu (E.R.K.); vadlamudi@uthscsa.edu (R.K.V.)
2 Department of Biochemistry, University of Wisconsin-Madison, Madison, WI 53706, USA; jjoshi6@wisc.edu
3 Greehey Children's Cancer Research Institute, University of Texas Health San Antonio, San Antonio, TX 78229, USA; cheny8@uthscsa.edu (Y.C.); laiz@uthscsa.edu (Z.L.)
4 Department of Population Health Sciences, University of Texas Health San Antonio, San Antonio, TX 78229, USA
5 Department of Molecular Medicine, University of Texas Health San Antonio, San Antonio, TX 78229, USA
6 Evestra, Inc., San Antonio, TX 78245, USA; bsanthamma@evestra.com (B.S.); hnair@evestra.com (H.B.N.)
7 Mays Cancer Canter, University of Texas Health San Antonio, San Antonio, TX 78229, USA
8 Audie L. Murphy Division, South Texas Veterans Health Care System, San Antonio, TX 78229, USA
* Correspondence: subbarayalu@uthscsa.edu (P.S.); viswanadhapa@uthscsa.edu (S.V.); Tel.: +1-(210)-562-9140 (P.S.); +1-(210)-458-3073 (S.V.)

Simple Summary: The obesity epidemic in the USA is increasing the risk of aggressive triple-negative breast cancer (TNBC) in obese women. This study investigated the potential impact of obesity on the advancement of TNBC by amplifying leukemia inhibitory factor receptor (LIFR) signaling. We tested the effects of LIFR inhibition using EC359 on TNBC cells in obesity conditions. The obesity environment increased TNBC cell growth and invasion, and treatment with EC359 effectively reduced these effects. Using TNBC cells, patient-derived organoids, and mouse models, we showed that EC359 can inhibit obesity-linked TNBC progression. Collectively, our results suggest targeting LIFR signaling as a potential treatment for obesity-related TNBC.

Abstract: American women with obesity have an increased incidence of triple-negative breast cancer (TNBC). The impact of obesity conditions on the tumor microenvironment is suspected to accelerate TNBC progression; however, the specific mechanism(s) remains elusive. This study explores the hypothesis that obesity upregulates leukemia inhibitory factor receptor (LIFR) oncogenic signaling in TNBC and assesses the efficacy of LIFR inhibition with EC359 in blocking TNBC progression. TNBC cell lines were co-cultured with human primary adipocytes, or adipocyte-conditioned medium, and treated with EC359. The effects of adiposity were measured using cell viability, colony formation, and invasion assays. Mechanistic studies utilized RNA-Seq, Western blotting, RT-qPCR, and reporter gene assays. The therapeutic potential of EC359 was tested using xenograft and patient-derived organoid (PDO) models. The results showed that adipose conditions increased TNBC cell proliferation and invasion, and these effects correlated with enhanced LIFR signaling. Accordingly, EC359 treatment reduced cell viability, colony formation, and invasion under adipose conditions and blocked adipose-mediated organoid growth and TNBC xenograft tumor growth. RNA-Seq analysis identified critical pathways modulated by LIF/LIFR signaling in diet-induced obesity mouse models. These findings suggest that adiposity contributes to TNBC progression via the activation of the LIF/LIFR pathway, and LIFR inhibition with EC359 represents a promising therapeutic approach for obesity-associated TNBC.

Keywords: EC359; obesity; TNBC; LIF/LIFR signaling; RNA-seq

check for updates

Citation: Randolph, L.; Joshi, J.; Rodriguez Sanchez, A.L.; Pratap, U.P.; Gopalam, R.; Chen, Y.; Lai, Z.; Santhamma, B.; Kost, E.R.; Nair, H.B.; et al. Significance of LIF/LIFR Signaling in the Progression of Obesity-Driven Triple-Negative Breast Cancer. *Cancers* **2024**, *16*, 3630. https://doi.org/10.3390/cancers16213630

Academic Editors: Zaklina Kovacevic and Ramadevi Subramani

Received: 11 August 2024
Revised: 20 September 2024
Accepted: 17 October 2024
Published: 28 October 2024

Copyright: © 2024 by the authors. Licensee MDPI, Basel, Switzerland. This article is an open access article distributed under the terms and conditions of the Creative Commons Attribution (CC BY) license (https://creativecommons.org/licenses/by/4.0/).

1. Introduction

Triple-negative breast cancer (TNBC), a subtype of breast cancer that lacks estrogen, progesterone, and HER2 receptors, accounts for 15–20% of BC cases and contributes disproportionately to BC mortality due to a lack of targeted therapies [1,2]. The incidence of TNBC is higher in obese women and obese TNBC patients exhibit a larger tumor size, higher grade, and stage [3,4]. Obesity is an independent risk factor that increases the risk of TNBC progression, therapy resistance, and metastases [5,6]. The currently available targeted therapies are only useful in a subset of TNBC patients with mutations (such as BRCA1). While chemotherapy has proved effective in some TNBC patients, therapy resistance and relapse are very common and thus limit the utility of chemotherapy. New targeted therapies are needed for the efficient management of TNBC.

Obesity-driven signaling functions as a potent inducer of the leukemia inhibitory factor (LIF), the most pleiotropic member of the interleuki-6 family of cytokines [7]. The LIFR-gp130 complex mediates LIFR signaling [8]. LIFR does not have inherent tyrosine kinase activity. LIFR and gp130 constitutively connect with the JAK-Tyk family of cytoplasmic tyrosine kinases, and LIF binding to the LIFR complex activates JAK, STAT, MAPK, AKT, and mTOR [8–10]. LIF and its receptor LIFR are commonly over-expressed in multiple solid tumors [11] and tumors upregulate LIF/LIFR signaling via autocrine and paracrine mechanisms [12–14]. LIF/LIFR signaling plays a key role in tumor growth, progression, metastasis, stemness, and therapy resistance [10,15–17]. LIF/LIFR activation occurs more prominently in TNBC compared to estrogen receptor positive (ER^+) BC, and high circulating LIF levels correlate with tumor recurrence and contribute to chemoresistance [14,18]. However, the role of LIF/LIFR signaling in the progression of obesity-driven TNBC remains elusive.

Recent studies suggested that the LIF/LIFR axis represents a potential therapeutic target. A LIF blockade or genetic LIFR deletion slow tumor progression and augment the efficacy of chemotherapy [16]. Another study confirmed that the blockade of LIF improves the therapeutic outcome [17]. With our expertise in developing novel small-molecule inhibitors, we have rationally designed and synthesized a small organic molecule that can emulate the LIF–LIFR binding site and functions as a LIFR inhibitor (EC359) [19]. EC359 represents a first-in-class drug to inhibit LIFR oncogenic functions. In this study, we tested the hypothesis that obesity enhances LIFR signaling in TNBC, contributing to cancer progression, and tested the therapeutic potential of LIFR inhibition using the small-molecule inhibitor EC359.

2. Materials and Methods

2.1. Cell Culture and Reagents

TNBC cell lines (MDA-MB-231, BT-549, SUM159, and 4T1) were purchased from ATCC and were maintained using ATCC-recommended medium. Human primary mature adipocytes (ADP) were isolated from subcutaneous fat samples obtained from UT Health ObGyn tissue core that obtained these tissues with informed consent using approved IRB protocol. In this study, we used six distinct adipose tissue samples, labeled ADP-1 through ADP-6. Conditioned medium collected to form these tissue samples was named as ADP-CM-1-to-6. Each sample was obtained from a different individual with a Body Mass Index (BMI) exceeding 30, ensuring that the samples were representative of individuals with obesity for our analysis. Adipocyte-conditioned medium (ADP-CM) was prepared by incubating 2 mL of packed primary mature adipocytes in 6 mL of serum-free DMEM medium in a 100 cm^2 petri dish for 48 h. In all in vitro experiments, basal DMEM medium was used as serum-free medium (SFM) and was combined with 50% (v/v) ADP-CM. The synthesis of LIFR inhibitor EC359 was earlier described [19].

2.2. Co-Culture and Treatment Conditions

Mature adipocytes were cultured in DMEM supplemented with 0.5% FBS. For the co-culture experiment, 1 mL of packed primary mature adipocytes was added to an insert in a

Boyden chamber, while MDA-MB-231 cells were seeded in the bottom well of a 6-well plate. Control wells had the insert without mature adipocytes. The co-cultures were performed in triplicate for 24 h with or without EC359 (100 nM) treatment. Following this, MDA-MB-231 cells were lysed to isolate proteins for Western blot analysis.

2.3. Cell Viability, Colony Formation, and Invasion Assays

For cell viability assays, TNBC cells were seeded at a density of 1×10^3 cells per well in a 96-well plate and incubated with ADP-CM, with or without EC359 at concentrations of 100 and 50 nM. After five days of drug treatment, cell viability was assessed using the MTT assay. Colony formation was evaluated by seeding cells at low density (500 cells per well) and culturing them with ADP-CM and EC359 (50 nM), the medium was replaced with regular cell culture medium, and the cells were cultured for an additional 14 days to allow colonies to form. The colonies developed during long-term culture were then counted. Invasion assays were performed using Matrigel-coated Transwell chambers as described [19]. For these assays, 100,000 cells were plated in the upper chamber with or without ADP-CM and with or without EC359 (100 nM), while regular cell culture medium was added to the lower chamber. After 22 h of incubation, the cells that had invaded through the Matrigel were stained with 0.5% crystal violet. The number of invaded cells was then counted per microscopic field.

2.4. Generation of LIFR-Knockdown Cells

MDA-MB-231/STAT3/luc cells were transfected using Lipofectamine RNAiMAX Reagent (Thermo Fisher, Waltham, MA, USA; cat# 13778150) following the manufacturer's instructions. Cells were transfected with either scrambled siRNA (siRNA Universal Negative Control #1) or LIFR-targeting siRNAs (siLIFR-1 and siLIFR-2) from Sigma-Aldrich (St. Louis, MO, USA). Specifically, siLIFR-1 corresponds to the LIFR siRNA ID SASI_Hs02_00330114, and siLIFR-2 corresponds to SASI_Hs02_00330115. Transfection was allowed to proceed for 72 h, after which the cells were analyzed by STAT3 reporter assay.

2.5. Western Blotting and RT-qPCR

RT-qPCR analysis was used to determine mRNA levels and Western blotting was used to evaluate protein expression, using standard protocols [19]. The antibodies used in this study were p-p70S6K(T389), p70S6K, p-Akt(S473), Akt, p-mTOR(S2448), mTOR, p-S6(S235/236), S6, p-ERK1/2, ERK, p-STAT3(Y705), and STAT3, which were purchased from Cell Signaling Technology (Beverly, MA, USA), the LIF and LIFR were acquired from Santa Cruz Biotechnology (Dallas, TX, USA), and anti-β-actin from Sigma (St. Louis, MO, USA). Using a CFX96 Real-Time PCR instrument and a High-Capacity cDNA Reverse Transcription Kit and PowerUp SYBR Green master mix (Applied Biosystems, Foster City, CA, USA), RT-qPCR was performed. Supplementary Table S1 has primer sequences and Figures S1 and S2 in Supplementary data have the original Western blots.

2.6. Reporter Gene Assays

STAT3 reporter gene assays were conducted as described previously [19]. Briefly, STAT3-luc reporter cells were deprived of serum for 24 h, followed by treatment with either ADP-CM alone or ADP-CM combined with EC359 for another 24 h. The activity of the reporter was then measured using a luminometer and the luciferase reporter assay system (Promega, Madison, WI, USA).

2.7. Obesity Induction

For diet-induced obesity studies, Rodent diet with 60 kcal% fat was used for high-fat-diet (HFD) groups (Research Diets, Inc., #D12492 New Brunswick, NJ, USA) and for low-fat-diet (LFD) groups, rodent diet with 10 kcal% fat was used (Research Diets, Inc. #D12450J New Brunswick, NJ, USA). Body weight was monitored weekly twice.

2.8. Xenograft and Patient-Derived Organoid Models

TNBC xenografts were established by injecting MDA-MB-231 into the mammary fat pad of immunocompromised SCID mice, with or without co-implantation of adipocytes or with low-fat-diet (LFD)/high-fat-diet (HFD) feeding. All animal experiments were conducted using approved UT Health San Antonio IACUC protocol and guidelines. For adiposity-driven studies, MDA-MB-231 cells and mature ADP cells (1×10^6) were mixed with equal volume of growth factor-reduced Matrigel and injected orthotopically into 8-week-old female SCID mice (n = 7 tumors/group). For diet-induced obesity studies, female SCID mice (n = 5/group) were fed with HFD or LFD. After 8 weeks, mice were implanted with MDA-MB-231 cells (1×10^6 cells in 100 µL), mixed with an equal volume of growth-factor-reduced Matrigel, in the mammary fat pads. After tumor establishment, mice were randomized into control and treatment groups. The control group received vehicle (0.3% hydroxy propyl cellulose) and the treatment group received EC359 (5 mg/kg/ip/5 days/week). All mice were monitored daily for adverse toxic effects. Tumor growth was measured with a caliper at 3–4-day intervals, and volume was calculated using a modified ellipsoidal formula: tumor volume = $1/2(L \times W^2)$, where L is the longitudinal diameter and W is the transverse diameter. At the end of the experiment, mice were euthanized, and tumors were excised and weighed.

For patient-derived organoid ex vivo models, mice bearing TNBC PDX (TM00096) tumors were purchased from Jackson laboratory (Bar Harbor, ME, USA). When tumors reached ~750 mm^3 size, they were dissected into small pieces, digested with collagenase, and were cultured as previously described [20]. For cell viability assays, 5×10^3 cells in a 10 µL droplet were seeded into each well of a 96-well plate. Organoid cultures were treated with EC359 or vehicle control, with or without ADP-CM, in triplicate. After 7 days of treatment, cell viability was assessed using the Promega® CellTiter-Glo® 3D-Superior Cell Viability Assay reagent according to the manufacturer's instructions (Promega, Madison, WI, USA). Luminescence intensity was measured using a GloMax® Discover System (Promega, Madison, WI, USA).

2.9. Syngeneic Xenograft Model

After 6 weeks of diet initiation with either LFD or HFD, 5×10^5 4T1 cells were injected orthotopically, in a total volume of 100 µL, into the mammary fat pad of BALB/c mice. All animals continued to be fed their respective diets until euthanasia. Tumor volume was measured using a digital caliper and calculated using a modified ellipsoidal formula: tumor volume = $1/2(L \times W2)$, where L is the longitudinal diameter and W is the transverse diameter. After euthanasia, tumors, fat tissue, spleen, and liver were collected and weighed.

2.10. RNA-Seq Analysis

Total RNA was isolated using RNeasy mini kit (Qiagen, Valencia, CA, USA) from 4T1 syngeneic xenograft tissues. The effect of LFD, HFD, and HFD + EC359 treatment on the global transcriptome was determined. The UT Health genome sequencing core facility sequenced RNA. The sequence data were aligned to the mouse genome (UCSC mm9) using TopHat2. HTSeq quantified genes and NCBI RefSeq annotated them. DESeq identified differentially expressed genes [21]. Genes having a fold change larger than 2 and a multiple-test-adjusted *p*-value below 0.01 were used for pathway analysis. GSEA [22] was conducted on 16 October 2023.

2.11. Statistical Analysis

Data were analyzed using GraphPad Prism software (version 9.5.1. Dotmatics, Boston, MA, USA). Statistical significance was determined by ANOVA or *t*-test, with $p < 0.05$ considered significant.

3. Results

3.1. Adipose Conditions Promote TNBC Cell Proliferation and LIFR Downstream Signaling

TNBC cells (BT-549 and SUM-159) were cultured in adipocyte-conditioned medium (ADP-CM) for 24 h. The expression of LIFR target genes was assessed using RT-qPCR. Under conditions of obese-related adiposity, there was a significant upregulation of LIFR target genes in both BT-549 and SUM-159 cells compared to control conditions (Figure 1A,B). Western blot analysis revealed increased expression or activation of LIFR downstream signaling proteins in TNBC cells treated with ADP-CM compared to untreated cells (Figures 1C, S1 and S3A). Collectively, these results suggest that ADP-CM enhances LIFR downstream signaling at the protein level, corroborating the gene expression data from RT-qPCR.

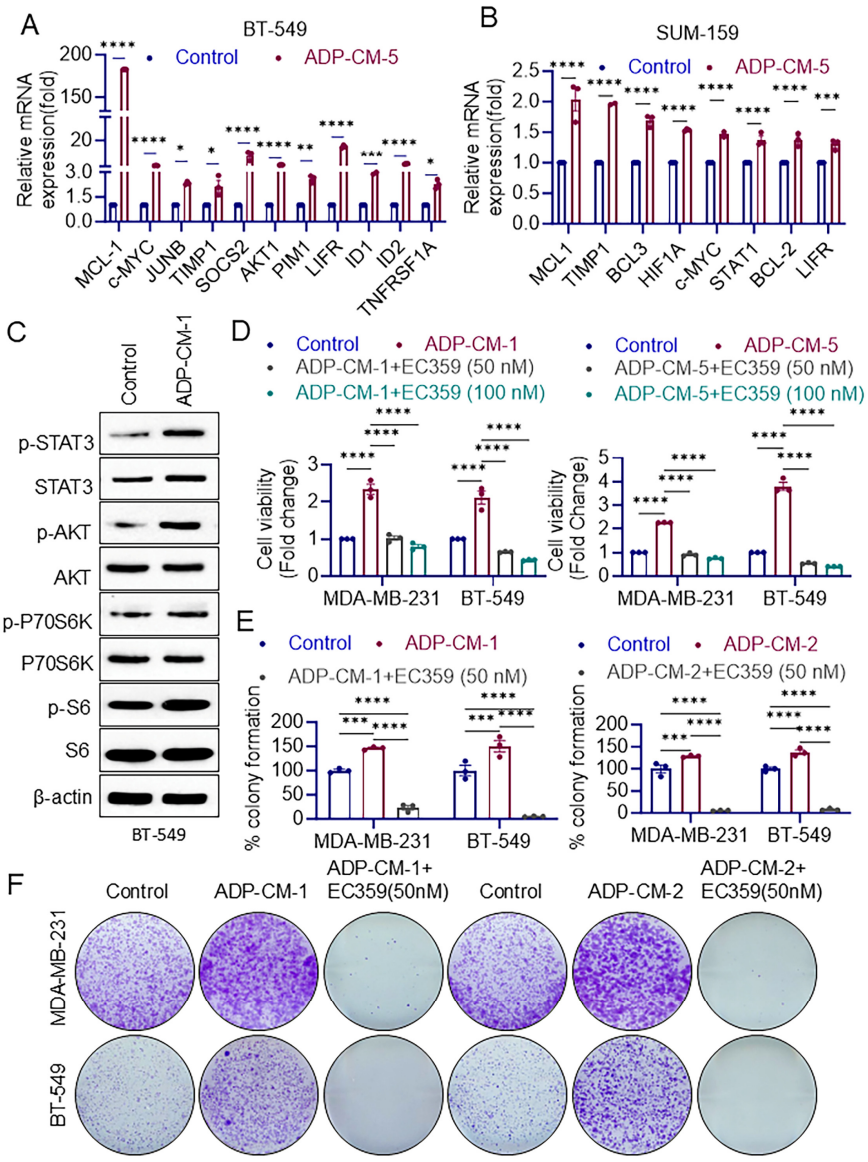


Figure 1. Obese-related adiposity conditions enhance LIFR downstream signaling. TNBC cells, BT-549 (**A**), and SUM-159 (**B**) were cultured with ADP-CM for 24 h, and the expression of LIFR target genes was analyzed by RT-qPCR. (**C**) TNBC cells cultured with ADP-CM for 24 h were analyzed using Western blot analysis to measure LIFR downstream signaling proteins. (**D**) The effects of EC359 treatment against adipose conditions on TNBC cell viability were determined using MTT assays. (**E**) The effects of ADP-CM and ADP-CM + EC359 (50 nM) on adiposity-induced cell survival of TNBC cells was measured using colony formation assays. (**F**) Representative images of colonies were shown. ns, not significant; * $p < 0.05$; ** $p < 0.01$; *** $p < 0.001$; **** $p < 0.0001$.

3.2. LIFR Inhibition with EC359 Suppresses TNBC Cell Growth

TNBC cells were treated with EC359 both with and without the presence of adipose conditions (ADP-CM), and cell viability was assessed using MTT assays. The results demonstrated that EC359 treatment significantly decreased TNBC cell viability compared to untreated cells under adipose (ADP-CM) and non-adipose conditions (Figures 1D, S4A,B and S5A). Further, cells treated with ADP-CM alone showed enhanced colony formation, indicating increased cell survival under adipose conditions (Figures 1E,F and S5C,D). Addition of EC359 to ADP-CM significantly reduced the number of colonies formed compared to ADP-CM alone. Collectively, these results suggest that EC359 attenuates adiposity-induced cell survival in TNBC cells (Figures 1E,F and S5C,D).

3.3. EC359 Inhibits LIFR Downstream Signaling

To evaluate LIFR downstream signaling, we have initially measured STAT3 reporter activity under adipose (ADP-CM) and non-adipose conditions. The results showed that ADP-CM significantly increased STAT3 reporter activity. The presence of EC359 effectively decreased STAT3 reporter activity both with and without the presence of adipose conditions (ADP-CM), suggesting that EC359 inhibits LIFR signaling pathway activation (Figures 2A, S4C and S5E). To provide direct evidence that the increase in STAT3 reporter activity is initiated primarily through LIFR signaling, we have knocked down LIFR using two distinct siRNAs. Western blotting confirmed the knock down of LIFR. Interestingly, when we knocked down LIFR using two distinct siRNAs, ADP-CM was not able to increase the STAT3 reporter activity (S4D–F). These results, taken together with the data in Figure 2A, support that ADP-CM-mediated increases in the STAT3 activity occur primarily via LIFR signaling.

ADP-CM treatment also led to the elevated expression of LIFR target genes in both BT-549 and MDA-MB-231 cells (Figure 2B). When EC359 was added, the expression of these target genes was significantly reduced compared to cells treated with ADP-CM alone (Figure 2B). In MDA-MB-231 cells, Western blot analyses revealed that ADP-CM treatment increased the levels of phospho-STAT3, while EC359 treatment reduced these levels, further demonstrating that EC359 inhibits LIFR signaling pathway activation (Figures 2C, S2A and S3B). We then used coculture assays to test the EC359 effect. MDA-MB-231 cells were co-cultured with adipocytes using a transwell system in the presence or absence of EC359 for 24 h. A Western blot analysis of these cells revealed that co-culturing with adipocytes enhanced LIFR downstream signaling activation. However, EC359 attenuated this activation (Figures 2D, S2B and S3C). To explore the impact of EC359 on the obesity-induced invasion of TNBC cells, Matrigel invasion assays were performed. EC359 significantly reduced the invasion potential of TNBC cells under ADP-CM conditions (Figure 2E,F). In summary, these results demonstrate that obesity conditions enhance LIFR downstream signaling and increase invasion in TNBC cells, as evidenced by increased STAT3 reporter activity, increased LIFR target gene expression, elevated levels of signaling proteins, and enhanced invasion. EC359 effectively mitigates these effects, highlighting its potential as a therapeutic agent for inhibiting LIFR signaling pathway activation in TNBC cells exposed to adipose conditions.

3.4. EC359 Inhibits Obesity-Induced Growth in Organoid and Xenograft Models

EC359 treatment significantly inhibited the growth of TNBC patient-derived organoids cultured under adipose conditions (Figure S5B). To test the efficacy of EC359 in vivo, we have used xenograft models. MDA-MB-231 cells, along with mature adipocytes mixed in Matrigel were injected into the mammary fat pad of female SCID mice. Once tumors were established, the mice were randomized into control and EC359 treatment groups. The co-implantation of Adipocytes with TNBC cells enhanced TNBC progression, resulting in larger tumors with an increased volume and weight. EC359 treatment abolished obesity-induced TNBC progression (Figures 3A,B and S6A).

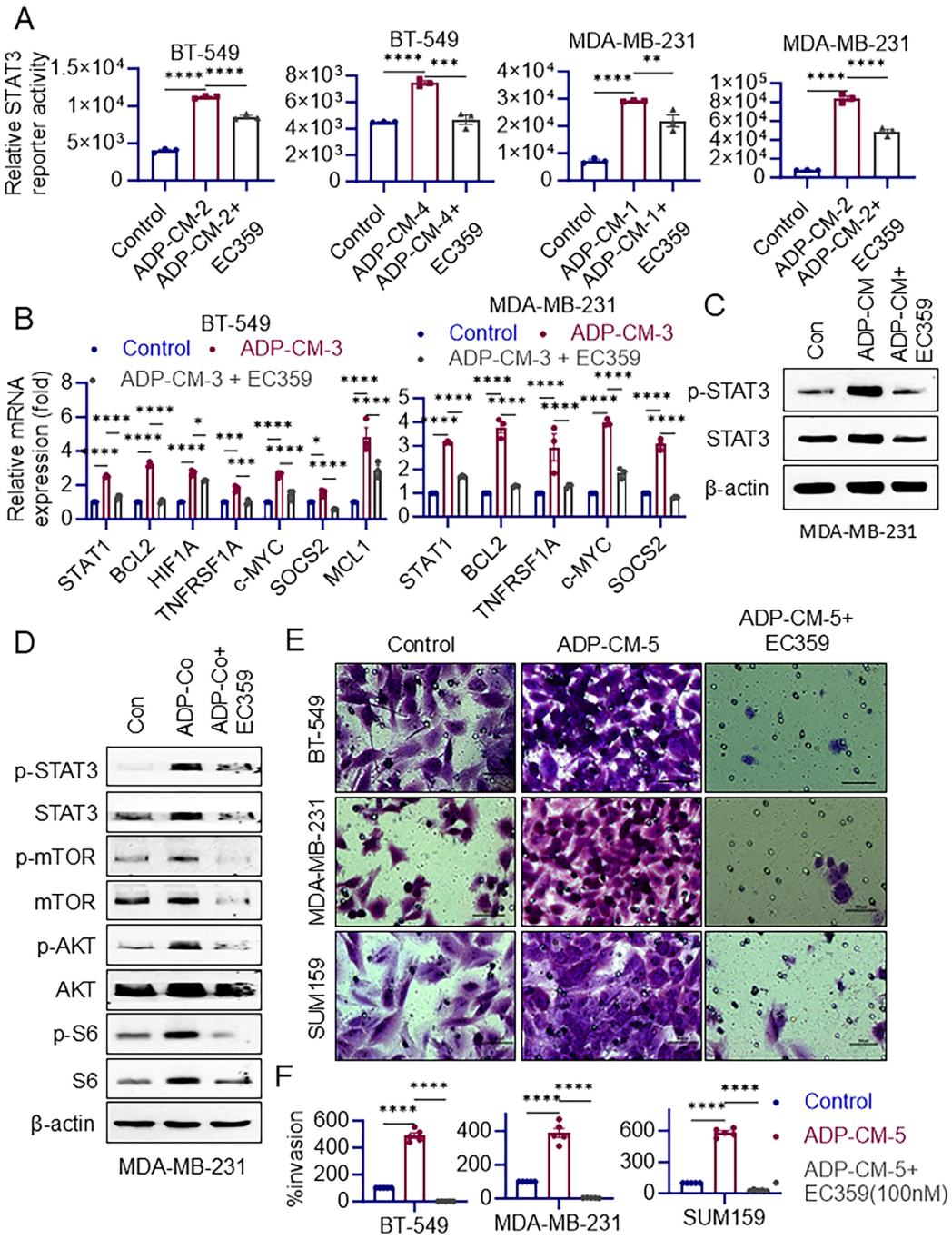


Figure 2. ADP-CM or co-culture of adipocytes enhances LIFR downstream signaling in TNBC and addition of EC359 (100 nM) reduces its activity in vitro. TNBC cells that stably express the STAT3 reporter were used. ADP-CM (**A**) activates STAT3 reporter activity, with EC359 (100 nM) effectively reducing STAT3 activity in ADP-CM conditions. (**B**) BT-549 and MDA-MB-231 cells were cultured with ADP-CM in the presence or absence of EC359 (100 nM) for 24 h, and the expression of LIFR target genes was analyzed by RT-qPCR. (**C**) MDA-MB-231 cells were incubated with or without ADP-CM and EC359 (100 nM) and were analyzed using Western blot analysis to measure LIFR downstream signaling proteins. (**D**) Adipocytes were indirectly co-cultured with MDA-MB-231 cells using a transwell culture system in the presence or absence of EC359 (100 nM) for 24 h. Signaling was profiled by Western blotting. (**E**) Effect of adipose conditions on TNBC cell invasion in the presence or absence of EC359 (100 nM) was determined by Boyden chamber assay and invaded cells were quantified (**F**). * $p < 0.05$; ** $p < 0.01$; *** $p < 0.001$; **** $p < 0.0001$.

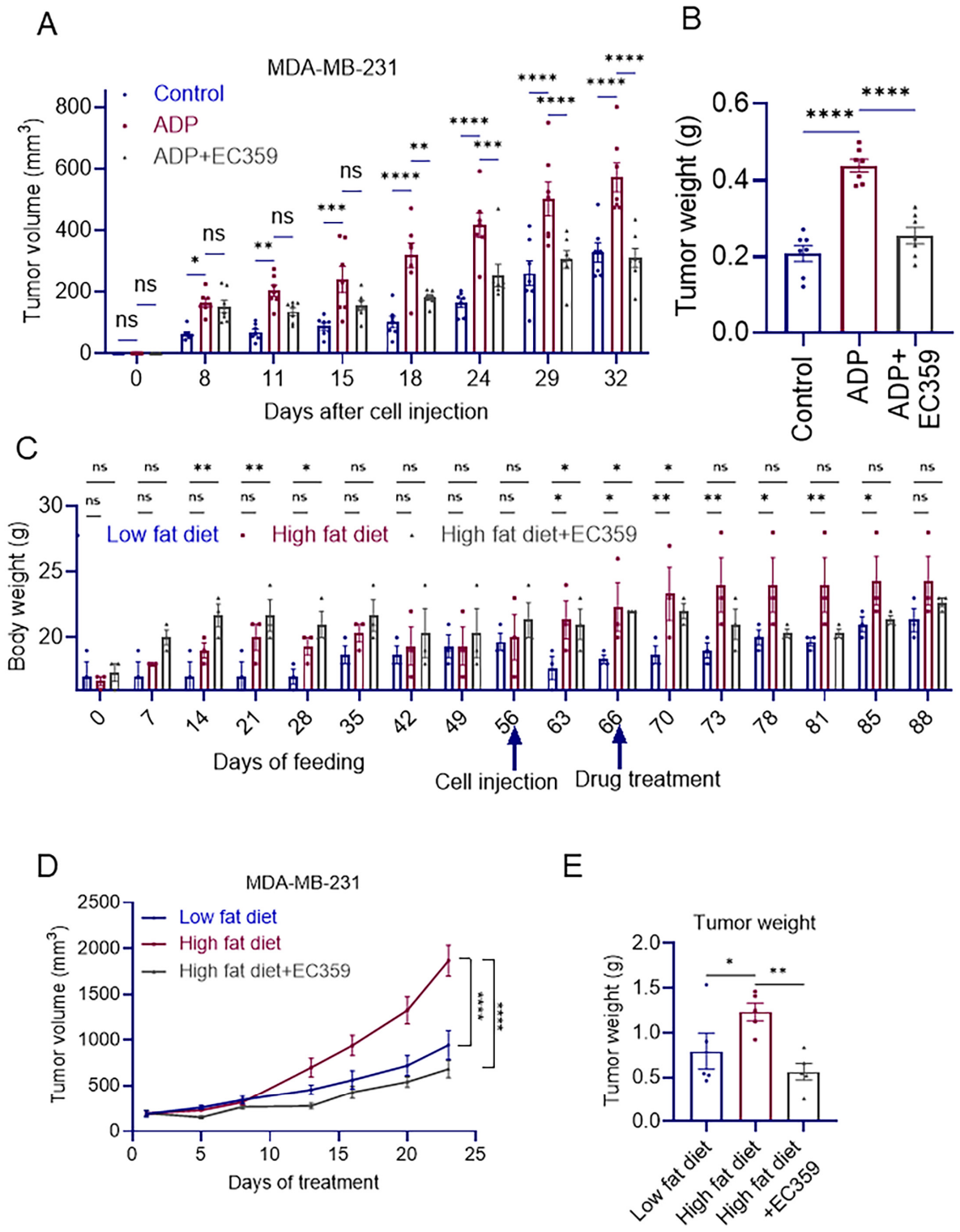


Figure 3. EC359 reduces tumor volume and weight in adiposity and diet-induced TNBC CDX models. Primary human adipose cells were co-implanted with MDA-MB-231 cells via orthotopic injection (n = 7) and subsequently treated with or without EC359 (5 mg/kg, intraperitoneally, 5 days per week). Tumor volumes (**A**) and tumor weights (**B**) are shown in graph. (**C**) Body weights of Low-fat-diet- and high-fat-diet-induced TNBC xenograft models treated with or without EC359 (5 mg/kg/ip/5 days/week) are shown in graph. Tumor volume (**D**) and tumor weights (**E**) are shown. ns, not significant; * $p < 0.05$, ** $p < 0.01$, *** $p < 0.001$, **** $p < 0.0001$.

We next investigated the effects of an HFD on inducing obesity and subsequent TNBC tumor progression in female SCID mice, followed by treatment with EC359 to determine if it could counteract obesity-induced TNBC progression. The mice were randomized into three groups: LFD, HFD, and HFD + EC359. The LFD group was fed a 10% low-fat diet, while the HFD groups were fed a 60% high-fat diet for eight weeks. Body weights were monitored twice a week. After eight weeks, MDA-MB-231 cells mixed with Matrigel (1.0×10^6 cells in 100 µL) were injected into the mammary fat pads of the mice. Following tumor establishment, mice on the HFD had increased body weights compared to those on the 10% low-fat diet (Figure 3C). HFD significantly enhanced tumor growth, which is attenuated by EC359 treatment (Figures 3D,E and S6B).

3.5. EC359 Inhibits High-Fat-Diet-Induced Syngeneic Xenograft Tumor Growth

To further confirm the utility of EC359 in blocking the obesity-mediated growth of TNBC cells in vivo, we used 4T1 cells in a syngeneic BALB/c mice model. We first fed BALB/c mice with a LFD and HFD for six weeks. After this period, 4T1 cells were injected orthotopically into the mammary fat pad of both groups. Once tumors formed, the mice were randomized into three groups: (1) LFD, (2) HFD, and (3) HFD + EC359. As shown in Figure 4A–G, mice fed with the HFD exhibited significantly enhanced 4T1 xenograft tumor growth. Additionally, treatment with EC359 significantly attenuated HFD-induced TNBC progression (Figure 4A–G).

To better understand the mechanisms by which obese conditions stimulate TNBC progression, we employed a global RNA-seq approach. For this experiment, we utilized tumor tissues from models fed with a LFD, HFD, and HFD with EC359 treatment. HFD-induced models significantly altered the expression of 578 genes compared to LFD models, and 325 genes were differentially expressed in the HFD + EC359 group compared to the HFD group. Gene set enrichment analysis (GSEA) revealed that genes regulated by the HFD group positively correlated with cytokine signaling pathways, stem cells, inflammation, TGFβ, metastasis, and epithelial–mesenchymal transition pathways (Figure 5A). These pathways were downregulated with EC359 treatment (Figure 5B). Functional analysis using Gene Ontology (NIH DAVID Bioinformatics tool https://david.ncifcrf.gov/tools.jsp (accessed on 1 August 2024) indicated that the upregulated biological processes in the HFD group included cell migration, proliferation, angiogenesis, cell chemotaxis, cell communication, and cell adhesion (Figure 5C), and these pathways were negatively enriched in the EC359-treated groups (Figure 5D). Among the 325 differentially expressed genes identified in the HFD + EC359 group compared to the HFD group, we refined our focus to those genes uniquely associated with the HFD by filtering out the genes overlapping with the LFD group. This analysis resulted in the identification of 179 differentially expressed genes, as shown in the Venn diagram and Heatmap. Subsequent DAVID analysis revealed that these genes were significantly associated with several key pathways related to cell–cell adhesion, the regulation of T cell differentiation, the apoptotic cleavage of cell adhesion proteins, the degradation of the extracellular matrix, the apoptotic cleavage of cellular proteins, and the canonical Wnt signaling pathway (Figures S7 and S8).

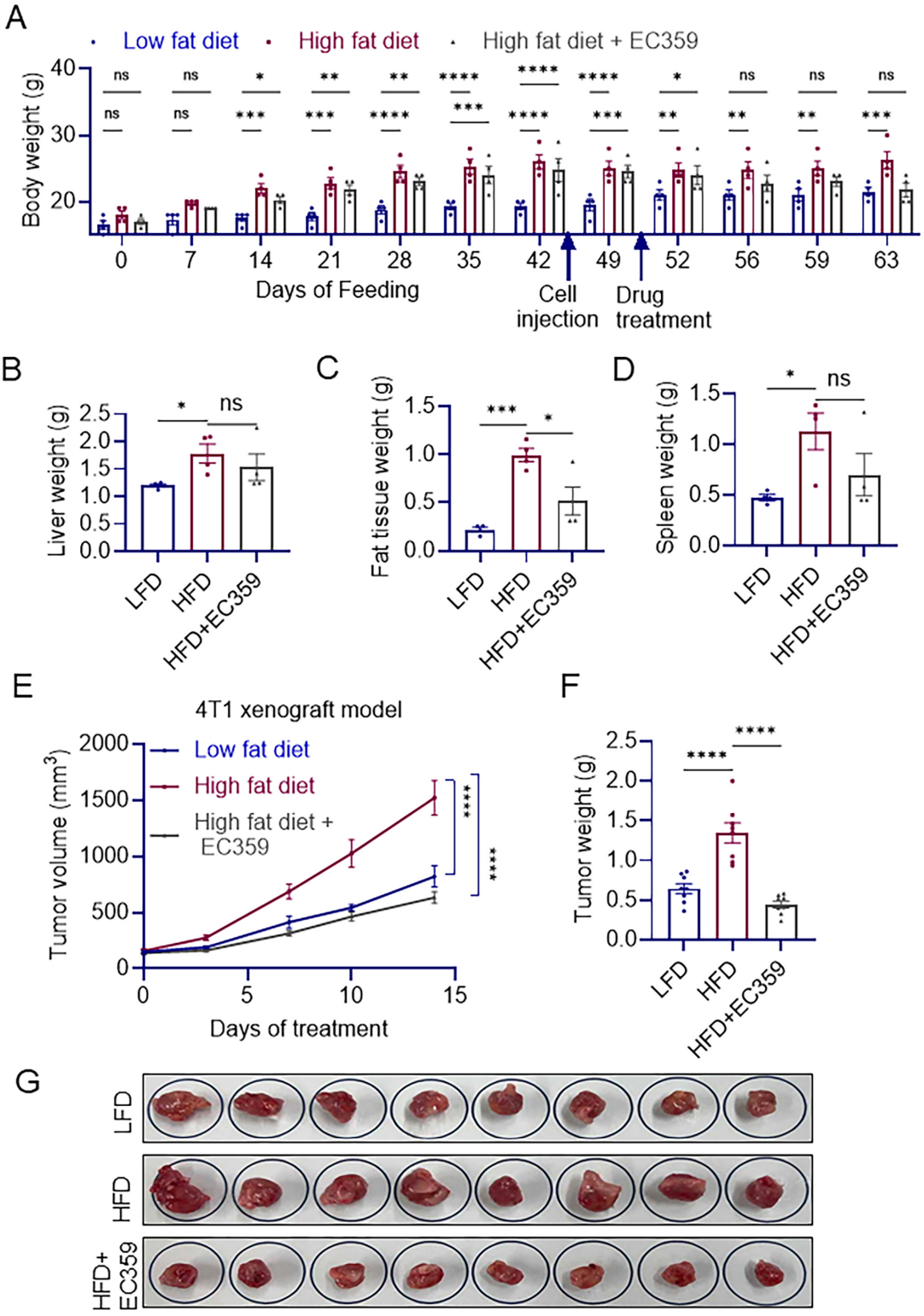


Figure 4. Low-fat diet and high-fat diet 4T1-TNBC syngeneic model. Diet-induced obesity syngeneic models (n = 8) were treated with vehicle or EC359 (5 mg/kg/ip/5 days/week). (**A**) Body weights shown in graph. Bar graphs of liver (**B**), fat tissue (**C**), spleen (**D**), and tumor volume (**E**) were shown. (**F**) Tumor weights of all the 3 groups are shown. (**G**) Representative images of excised tumors from diet-induced syngeneic xenografts treated with or without EC359. ns, not significant; * $p < 0.05$, ** $p < 0.01$, *** $p < 0.001$, **** $p < 0.0001$.

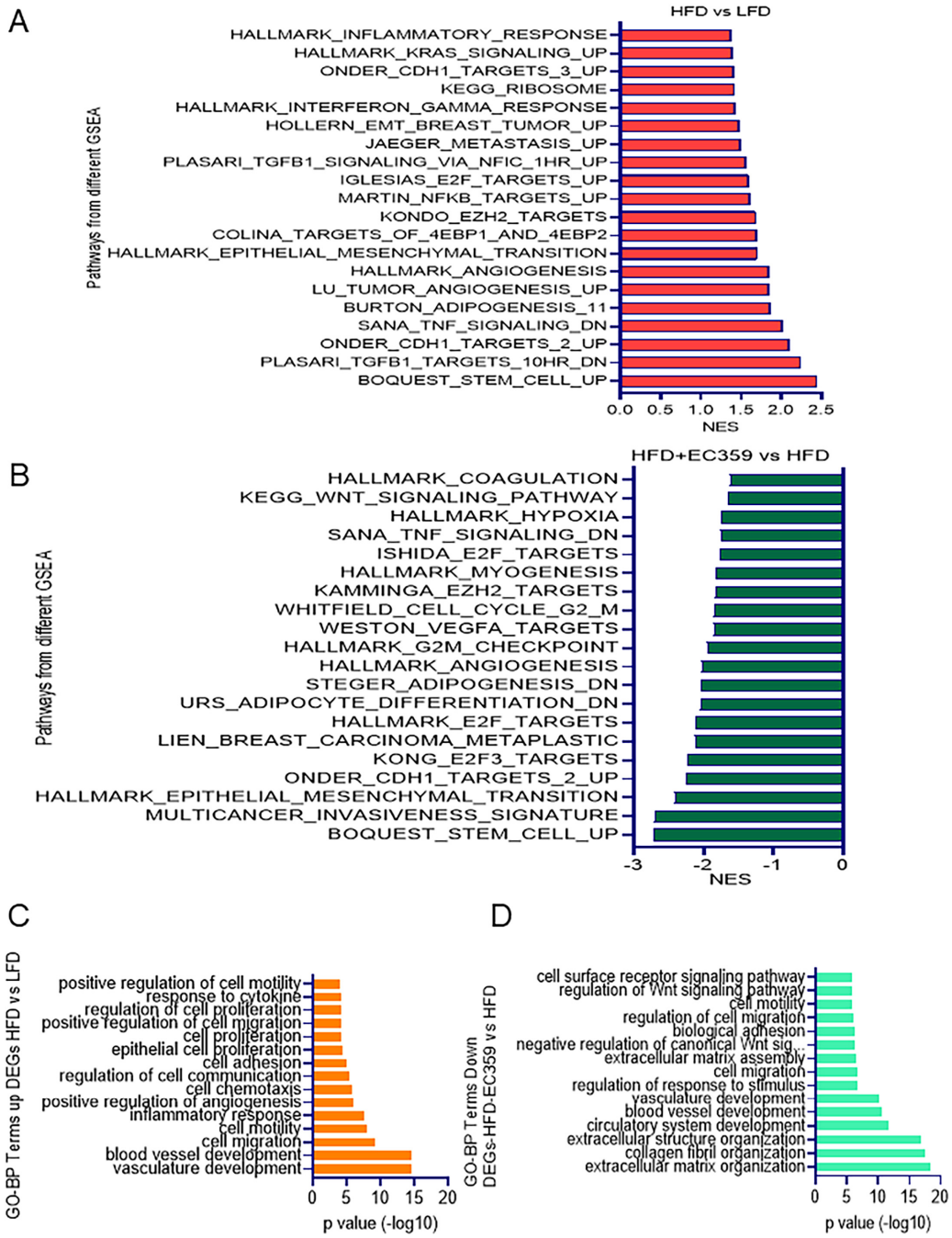


Figure 5. Differential gene expression analysis of TNBC syngeneic xenograft model. (**A**) GSEA reveals pathways with positive enrichment (upregulated pathways) in diet-induced obesity TNBC-4T1 syngeneic xenograft models after HFD feeding. (**B**) GSEA displays pathways with negative enrichment (downregulated pathways) in EC359-treated TNBC-4T1 syngeneic xenograft models after HFD feeding. Gene ontology analysis identifies biological processes with positive enrichment in HFD models (**C**) and negative enrichment in EC359-treated HFD models (**D**). Differentially expressed genes were filtered using log2FoldChange ≥ 2, and *p*adj < 0.01.

4. Discussion

Obesity is an independent risk factor [23] that increases the risk of TNBC progression [3,24] and metastases [25]. The prevalence of obesity in the USA has reached epidemic proportions, significantly impacting public health. Women with obesity are two times more likely to develop BC, with a 40% increased risk of cancer recurrence and death from

disease [5,26]. This study's findings demonstrate that the obesity-associated microenvironment promotes TNBC progression through the upregulation of LIFR signaling. Adipose conditions enhance TNBC cell proliferation and invasion, correlating with increased LIFR expression and the activation of STAT3 signaling. Importantly, the inhibition of LIFR with EC359 effectively blocks these oncogenic processes, suggesting that LIFR represents a potential therapeutic target for obesity-driven TNBC.

During the past 20 years, the obesity epidemic is rapidly increasing in USA and obese women are at a higher likelihood of developing TNBC [25]. Several studies implicated the importance of the breast microenvironment on aggressive cancer biology, especially the obese microenvironment [3,27]. However, the underlying mechanism(s) by which obesity contributes to the progression of TNBC remains unclear. The obesity microenvironment modulates cytokines [28] and is suspected to promote TNBC progression [3]. Obesity signals (such as leptin) function as potent inducers of the LIF [29,30], the most pleiotropic member of the interleukin-6 family of cytokines [7]. Our results demonstrated that TNBC cells cultured with ADP-CM showed the significant upregulation of LIFR target genes and increased activation of LIFR downstream signaling proteins. These findings indicate that the adipose environment enhances LIFR signaling, potentially promoting tumor progression in TNBC cells.

Published studies showed that tumors upregulate LIF/LIFR signaling via autocrine and paracrine mechanisms [12–14]. TNBC often exhibits the autocrine stimulation of the LIFR axis by altering the expression of ligands. For example, endoplasmic reticulum stress and hypoxia are a few of the hallmarks of TNBC [31] and hypoxia induces LIF expression in human cancer cells [32]. CircRNAs such as circSEPT9 regulate the expression of LIF via sponging miR-637 and activate the LIF/Stat3 signaling pathway involved in the progression of TNBC [33]. LIF promotes the proliferation and metastasis of BC cells, and the overexpression of LIF is commonly associated with poorer relapse free survival in BC patients [10]. Further, the increased expression of alternative LIFR ligands such as OSM, CNTF, and CTF1 was reported in TNBC [15]. Our findings are consistent with previous studies indicating the role of LIFR in cancer biology. Further, this study is the first to establish a direct link between obesity, LIFR signaling, and TNBC progression.

The LIF/LIFR axis is linked to cancer proliferation, immune system protection, chemoresistance, and patient survival [11,34,35]. Considering the significance of LIF/LIFR signaling in cancer, our team recently has created an inhibitor for LIFR, designated as EC359. The specificity of EC359 was determined by a microscale thermophoresis assay and LIFR knockdown cells [19]. EC359 exclusively targets cells that express LIF and LIFR. For example, EC359 shows little efficacy against ER^+ breast cancer cells, such as MCF7, which express minimal amounts of LIF and LIFR. Conversely, TNBC models like MDA-MB-231 exhibit elevated levels of LIF and LIFR, demonstrating significant responsiveness to EC359. Moreover, the depletion of LIFR in the TNBC model cells significantly diminished the efficacy of EC359 [19]. Toxicity investigations indicated no significant abnormalities in any of the treated animal groups at doses of up to 30 mg/kg and established 30 mg/kg as the maximum tolerated dose (MTD) [36]. Published studies showed the efficacy of EC359 in treating triple-negative breast cancer [19,37], endometrial cancer [20,38], pancreatic cancer [39,40], and renal cancer cells [41]. In this study, EC359 at a dosage of 5 mg/kg (which is substantially lower than the MTD dose) showed significant efficacy in mitigating the obesity-induced progression of TNBC. The use of EC359 to inhibit LIFR offers a novel therapeutic approach for managing obesity-associated TNBC, addressing a critical need for effective treatments in the TNBC population.

LIFR does not have inherent tyrosine kinase activity; LIF binding to the LIFR complex activates Jak-STAT as an immediate effector and MAPK, AKT, and mTOR as secondary effectors [8–10]. The LIF-STAT3 axis is implicated in stem cell self-renewal and pluripotency [42]. Our results show the suppression of STAT3 reporter activity and the reduced expression of LIFR target genes by EC359 further confirms its inhibitory effect on LIFR downstream signaling. The ability of EC359 to attenuate LIFR signaling in the presence of

ADP-CM, as well as in co-culture systems with adipocytes, indicates its broad applicability of targeting LIFR in disrupting obesity-enhanced signaling pathways in TNBC. The RNA-Seq analysis of xenograft models also confirmed critical pathways modulated by obesity via LIF/LIFR signaling, further elucidating the molecular mechanisms by which obesity influences TNBC progression. Collectively, our in vivo and ex vivo findings provide a strong rationale for considering EC359 in clinical settings to manage obesity-driven TNBC.

5. Conclusions

The results of this study have demonstrated the efficacy of EC359 in inhibiting the LIFR pathway and have established a critical function of LIFR signaling in mediating the effects of obesity on TNBC progression. EC359 is effective in reducing the proliferation and survival of TNBC cells driven by obesity in vitro, and it substantially impedes tumor growth in organoid and xenograft models. These results indicate that EC359 has the potential to be a therapeutic agent for the treatment of obesity-driven TNBC.

Supplementary Materials: The following supporting information can be downloaded at: https://www.mdpi.com/article/10.3390/cancers16213630/s1, Figure S1. Uncropped Western blots of Figure 1C. Figure S2. Uncropped Western blots of Figure 2C (A), and Figure 2D (B). Figure S3. The bar graphs represent the densitometric quantification of Figure 1C (A), Figure 2C (B), and Figure 2D (C) Western blots. Figure S4. The effects of EC359 treatment on TNBC cell viability (A,B) and STAT3 reporter activity (C) were determined by MTT and luciferase assays. D, The effectiveness of LIFR siRNA in reducing LIFR expression was demonstrated through Western blot analysis. E, F. The effect of ADP-CM on LIFR knockdown cells was evaluated through STAT3 reporter activity assays; Figure S5. The effects of EC359 treatment against adipose (A) conditions on TNBC cell viability were determined by MTT assays. Organoids generated from TNBC-PDX-96 were cultured in ADP-CM and treated with 1000 nM of EC359. B, Organoids viability of were measured after 7 days of treatment using CellTiter-Glo® 3D Cell Viability Assay. C, The effects of ADP-CM and ADP-CM+EC359 on adiposity-induced cell survival of TNBC cells was measured using colony formation assays. C, Representative images of colonies and its quantification (D) were shown. E, TNBC cells that stably express the STAT3 reporter were incubated with ADP-CM in the presence or absence of EC359 and the reporter activity was measured after 24 hrs.; Figure S6. A, MDA-MB-231 xenograft tumor images from control, ADP and ADP+EC359 were shown. B, MDA-MB-231 xenograft tumor images from LFD, HFD and HFD+EC359 were shown; Figure S7. A Venn diagram illustrating the overlapping differentially expressed genes (DEGs) among the 4T1 groups treated with LFD, HFD, and HFD + EC359, based on RNA-seq analysis; Figure S8. A heatmap displaying the uniquely upregulated and downregulated differentially expressed genes (DEGs) in comparisons between HFD versus LFD and HFD + EC359 versus HFD, based on RNA-seq analysis. Supplementary Table S1: List of primers used for the study.

Author Contributions: Conceptualization, P.S. and S.V.; methodology, L.R., J.J., A.L.R.S., U.P.P., R.G., P.S. and S.V.; Bio-informatic analysis, L.R., Y.C. and Z.L.; validation, L.R., R.K.V., P.S. and S.V.; formal analysis, L.R., U.P.P., R.G., P.S. and H.B.N.; investigation, R.K.V., P.S. and S.V.; resources, B.S., H.B.N. and E.R.K.; data curation L.R., J.J., A.L.R.S., U.P.P., P.S., R.K.V. and S.V.; writing—original draft preparation, L.R., R.K.V. and S.V.; writing—review and editing, L.R., U.P.P., P.S. and S.V.; supervision, R.K.V., P.S. and S.V.; funding acquisition, U.P.P., P.S., H.B.N., R.K.V. and S.V. All authors have read and agreed to the published version of the manuscript.

Funding: This research was funded by NIH-R01CA267893 (SV); ACS pilot grant IRG-21-147-01-IRG (SV); NIH R01 CA266970-01A1 (SV, RKV, HBN); Bank of America grant (UPP); NIH-R21-CA277164-01A1 (PS); VA1 I01 BX006280-0 1 (RKV); and NIH NCI R50 CA265339 (ZL). RNA-seq data were generated in the Genome Sequencing Facility, which is supported by UT Health San Antonio, NIH-NCI P30 CA054174 (Cancer Center at UT Health San Antonio), NIH Shared Instrument grant 1S10 OD030311-01 (S10 grant), and CPRIT Core Facility Award (RP220662).

Institutional Review Board Statement: This study used primary adipocytes obtained from the Ob Gyn tissue core. The core obtained these materials in accordance with the approved IRB methodology. This study was carried out in compliance with the Declaration of Helsinki and received approval from the Institutional Review Board of UT Health San Antonio (HSC20190695N and 09/03/2019).

The animal study protocol received approval from the Office of the Institutional Animal Care and Use Committee (Protocol number: 20220021AR) for research with animals.

Informed Consent Statement: Not applicable.

Data Availability Statement: All data generated for this study are included within this article. RNA-seq data have been deposited in the GEO database with a GEO accession number GSE280092.

Conflicts of Interest: Authors Bindu Santhamma and Hareesh B. Nair are current employees of Evestra Inc. All other remaining authors declare no competing interests.

References

1. Vagia, E.; Mahalingam, D.; Cristofanilli, M. The Landscape of Targeted Therapies in TNBC. *Cancers* **2020**, *12*, 916. [CrossRef] [PubMed]
2. Zagami, P.; Carey, L.A. Triple negative breast cancer: Pitfalls and progress. *npj Breast Cancer* **2022**, *8*, 95. [CrossRef] [PubMed]
3. Sun, H.; Zou, J.; Chen, L.; Zu, X.; Wen, G.; Zhong, J. Triple-negative breast cancer and its association with obesity. *Mol. Clin. Oncol.* **2017**, *7*, 935–942. [CrossRef] [PubMed]
4. Lohmann, A.E.; Soldera, S.V.; Pimentel, I.; Ribnikar, D.; Ennis, M.; Amir, E.; Goodwin, P.J. Association of Obesity With Breast Cancer Outcome in Relation to Cancer Subtypes: A Meta-Analysis. *J. Natl. Cancer Inst.* **2021**, *113*, 1465–1475. [CrossRef]
5. Jiralerspong, S.; Goodwin, P.J. Obesity and Breast Cancer Prognosis: Evidence, Challenges, and Opportunities. *J. Clin. Oncol.* **2016**, *34*, 4203–4216. [CrossRef]
6. Maguire, O.A.; Ackerman, S.E.; Szwed, S.K.; Maganti, A.V.; Marchildon, F.; Huang, X.; Kramer, D.J.; Rosas-Villegas, A.; Gelfer, R.G.; Turner, L.E.; et al. Creatine-mediated crosstalk between adipocytes and cancer cells regulates obesity-driven breast cancer. *Cell Metab.* **2021**, *33*, 499–512.e496. [CrossRef]
7. Nicola, N.A.; Babon, J.J. Leukemia inhibitory factor (LIF). *Cytokine Growth Factor. Rev.* **2015**, *26*, 533–544. [CrossRef]
8. Stahl, N.; Boulton, T.G.; Farruggella, T.; Ip, N.Y.; Davis, S.; Witthuhn, B.A.; Quelle, F.W.; Silvennoinen, O.; Barbieri, G.; Pellegrini, S.; et al. Association and activation of Jak-Tyk kinases by CNTF-LIF-OSM-IL-6 beta receptor components. *Science* **1994**, *263*, 92–95. [CrossRef]
9. Liu, S.C.; Tsang, N.M.; Chiang, W.C.; Chang, K.P.; Hsueh, C.; Liang, Y.; Juang, J.L.; Chow, K.P.; Chang, Y.S. Leukemia inhibitory factor promotes nasopharyngeal carcinoma progression and radioresistance. *J. Clin. Investig.* **2013**, *123*, 5269–5283. [CrossRef]
10. Li, X.; Yang, Q.; Yu, H.; Wu, L.; Zhao, Y.; Zhang, C.; Yue, X.; Liu, Z.; Wu, H.; Haffty, B.G.; et al. LIF promotes tumorigenesis and metastasis of breast cancer through the AKT-mTOR pathway. *Oncotarget* **2014**, *5*, 788–801. [CrossRef]
11. Zhang, C.; Liu, J.; Wang, J.; Hu, W.; Feng, Z. The emerging role of leukemia inhibitory factor in cancer and therapy. *Pharmacol. Ther.* **2021**, *221*, 107754. [CrossRef] [PubMed]
12. Kamohara, H.; Ogawa, M.; Ishiko, T.; Sakamoto, K.; Baba, H. Leukemia inhibitory factor functions as a growth factor in pancreas carcinoma cells: Involvement of regulation of LIF and its receptor expression. *Int. J. Oncol.* **2007**, *30*, 977–983. [CrossRef] [PubMed]
13. Shin, J.E.; Park, S.H.; Jang, Y.K. Epigenetic up-regulation of leukemia inhibitory factor (LIF) gene during the progression to breast cancer. *Mol. Cells* **2011**, *31*, 181–189. [CrossRef] [PubMed]
14. Morton, S.D.; Cadamuro, M.; Brivio, S.; Vismara, M.; Stecca, T.; Massani, M.; Bassi, N.; Furlanetto, A.; Joplin, R.E.; Floreani, A.; et al. Leukemia inhibitory factor protects cholangiocarcinoma cells from drug-induced apoptosis via a PI3K/AKT-dependent Mcl-1 activation. *Oncotarget* **2015**, *6*, 26052–26064. [CrossRef]
15. Doherty, M.R.; Parvani, J.G.; Tamagno, I.; Junk, D.J.; Bryson, B.L.; Cheon, H.J.; Stark, G.R.; Jackson, M.W. The opposing effects of interferon-beta and oncostatin-M as regulators of cancer stem cell plasticity in triple-negative breast cancer. *Breast Cancer Res.* **2019**, *21*, 54. [CrossRef]
16. Shi, Y.; Gao, W.; Lytle, N.K.; Huang, P.; Yuan, X.; Dann, A.M.; Ridinger-Saison, M.; DelGiorno, K.E.; Antal, C.E.; Liang, G.; et al. Targeting LIF-mediated paracrine interaction for pancreatic cancer therapy and monitoring. *Nature* **2019**, *569*, 131–135. [CrossRef]
17. Wang, M.T.; Fer, N.; Galeas, J.; Collisson, E.A.; Kim, S.E.; Sharib, J.; McCormick, F. Blockade of leukemia inhibitory factor as a therapeutic approach to KRAS driven pancreatic cancer. *Nat. Commun.* **2019**, *10*, 3055. [CrossRef]
18. Liu, J.; Yu, H.; Hu, W. LIF is a new p53 negative regulator. *J. Nat. Sci.* **2015**, *1*, e131.
19. Viswanadhapalli, S.; Luo, Y.; Sareddy, G.R.; Santhamma, B.; Zhou, M.; Li, M.; Ma, S.; Sonavane, R.; Pratap, U.P.; Altwegg, K.A.; et al. EC359: A First-in-Class Small-Molecule Inhibitor for Targeting Oncogenic LIFR Signaling in Triple-Negative Breast Cancer. *Mol. Cancer Ther.* **2019**, *18*, 1341–1354. [CrossRef]
20. Blankenship, L.; Pratap, U.P.; Yang, X.; Liu, Z.; Altwegg, K.A.; Santhamma, B.; Ramasamy, K.; Konda, S.; Chen, Y.; Lai, Z.; et al. Inhibition of LIFR Blocks Adiposity-Driven Endometrioid Endometrial Cancer Growth. *Cancers* **2022**, *14*, 5400. [CrossRef]
21. Anders, S.; Huber, W. Differential expression analysis for sequence count data. *Genome Biol.* **2010**, *11*, R106. [CrossRef] [PubMed]
22. Subramanian, A.; Tamayo, P.; Mootha, V.K.; Mukherjee, S.; Ebert, B.L.; Gillette, M.A.; Paulovich, A.; Pomeroy, S.L.; Golub, T.R.; Lander, E.S.; et al. Gene set enrichment analysis: A knowledge-based approach for interpreting genome-wide expression profiles. *Proc. Natl. Acad. Sci. USA* **2005**, *102*, 15545–15550. [CrossRef] [PubMed]
23. Picon-Ruiz, M.; Morata-Tarifa, C.; Valle-Goffin, J.J.; Friedman, E.R.; Slingerland, J.M. Obesity and adverse breast cancer risk and outcome: Mechanistic insights and strategies for intervention. *CA Cancer J Clin.* **2017**, *67*, 378–397. [CrossRef] [PubMed]

24. Chen, H.L.; Ding, A.; Wang, M.L. Impact of central obesity on prognostic outcome of triple negative breast cancer in Chinese women. *Springerplus* **2016**, *5*, 594. [CrossRef]
25. Sabol, R.A.; Bowles, A.C.; Cote, A.; Wise, R.; O'Donnell, B.; Matossian, M.D.; Hossain, F.M.; Burks, H.E.; Del Valle, L.; Miele, L.; et al. Leptin produced by obesity-altered adipose stem cells promotes metastasis but not tumorigenesis of triple-negative breast cancer in orthotopic xenograft and patient-derived xenograft models. *Breast Cancer Res.* **2019**, *21*, 67. [CrossRef]
26. Neuhouser, M.L.; Aragaki, A.K.; Prentice, R.L.; Manson, J.E.; Chlebowski, R.; Carty, C.L.; Ochs-Balcom, H.M.; Thomson, C.A.; Caan, B.J.; Tinker, L.F.; et al. Overweight, Obesity, and Postmenopausal Invasive Breast Cancer Risk: A Secondary Analysis of the Women's Health Initiative Randomized Clinical Trials. *JAMA Oncol.* **2015**, *1*, 611–621. [CrossRef]
27. Dietze, E.C.; Chavez, T.A.; Seewaldt, V.L. Obesity and Triple-Negative Breast Cancer: Disparities, Controversies, and Biology. *Am. J. Pathol.* **2018**, *188*, 280–290. [CrossRef]
28. Pasquin, S.; Sharma, M.; Gauchat, J.F. Cytokines of the LIF/CNTF family and metabolism. *Cytokine* **2016**, *82*, 122–124. [CrossRef]
29. Wang, T.S.; Gao, F.; Qi, Q.R.; Qin, F.N.; Zuo, R.J.; Li, Z.L.; Liu, J.L.; Yang, Z.M. Dysregulated LIF-STAT3 pathway is responsible for impaired embryo implantation in a Streptozotocin-induced diabetic mouse model. *Biol. Open* **2015**, *4*, 893–902. [CrossRef]
30. Gonzalez, R.R.; Rueda, B.R.; Ramos, M.P.; Littell, R.D.; Glasser, S.; Leavis, P.C. Leptin-induced increase in leukemia inhibitory factor and its receptor by human endometrium is partially mediated by interleukin 1 receptor signaling. *Endocrinology* **2004**, *145*, 3850–3857. [CrossRef]
31. Chen, X.; Iliopoulos, D.; Zhang, Q.; Tang, Q.; Greenblatt, M.B.; Hatziapostolou, M.; Lim, E.; Tam, W.L.; Ni, M.; Chen, Y.; et al. XBP1 promotes triple-negative breast cancer by controlling the HIF1alpha pathway. *Nature* **2014**, *508*, 103–107. [CrossRef] [PubMed]
32. Wu, L.; Yu, H.; Zhao, Y.; Zhang, C.; Wang, J.; Yue, X.; Yang, Q.; Hu, W. HIF-2alpha mediates hypoxia-induced LIF expression in human colorectal cancer cells. *Oncotarget* **2015**, *6*, 4406–4417. [CrossRef] [PubMed]
33. Zheng, X.; Huang, M.; Xing, L.; Yang, R.; Wang, X.; Jiang, R.; Zhang, L.; Chen, J. The circRNA circSEPT9 mediated by E2F1 and EIF4A3 facilitates the carcinogenesis and development of triple-negative breast cancer. *Mol. Cancer* **2020**, *19*, 73. [CrossRef] [PubMed]
34. Hanahan, D. Hallmarks of Cancer: New Dimensions. *Cancer Discov.* **2022**, *12*, 31–46. [CrossRef]
35. Jorgensen, M.M.; de la Puente, P. Leukemia Inhibitory Factor: An Important Cytokine in Pathologies and Cancer. *Biomolecules* **2022**, *12*, 217. [CrossRef]
36. Ebrahimi, B.; Viswanadhapalli, S.; Pratap, U.P.; Rahul, G.; Yang, X.; Pitta Venkata, P.; Drel, V.; Santhamma, B.; Konda, S.; Li, X.; et al. Pharmacological inhibition of the LIF/LIFR autocrine loop reveals vulnerability of ovarian cancer cells to ferroptosis. *npj Precis. Oncol.* **2024**, *8*, 118. [CrossRef]
37. Li, M.; Viswanadhapalli, S.; Santhamma, B.; Pratap, U.P.; Luo, Y.; Liu, J.; Altwegg, K.A.; Tang, W.; Liu, Z.; Li, X.; et al. LIFR inhibition enhances the therapeutic efficacy of HDAC inhibitors in triple negative breast cancer. *Commun. Biol.* **2021**, *4*, 1235. [CrossRef]
38. Tang, W.; Ramasamy, K.; Pillai, S.M.A.; Santhamma, B.; Konda, S.; Pitta Venkata, P.; Blankenship, L.; Liu, J.; Liu, Z.; Altwegg, K.A.; et al. LIF/LIFR oncogenic signaling is a novel therapeutic target in endometrial cancer. *Cell Death Discov.* **2021**, *7*, 216. [CrossRef]
39. Hall, B.R.; Cannon, A.; Thompson, C.; Santhamma, B.; Chavez-Riveros, A.; Bhatia, R.; Nair, H.B.; Nickisch, K.; Batra, S.K.; Kumar, S. Utilizing cell line-derived organoids to evaluate the efficacy of a novel LIFR-inhibitor, EC359 in targeting pancreatic tumor stroma. *Genes. Cancer* **2019**, *10*, 1–10. [CrossRef]
40. Di Giorgio, C.; Lupia, A.; Marchiano, S.; Bordoni, M.; Bellini, R.; Massa, C.; Urbani, G.; Roselli, R.; Moraca, F.; Sepe, V.; et al. Repositioning Mifepristone as a Leukaemia Inhibitory Factor Receptor Antagonist for the Treatment of Pancreatic Adenocarcinoma. *Cells* **2022**, *11*, 3482. [CrossRef]
41. Feng, C.-Z.; Li, N.-Z.; Hu, X.-B.; Xie, Y.-Y.; Huang, Q.-H.; Zhang, J.; Chen, Z.; Chen, S.-J.; Wang, F.; Sun, X.-J. The LIFR-targeting small molecules EC330/EC359 are potent ferroptosis inducers. *Genes Dis.* **2023**, *10*, 735–738. [CrossRef]
42. Cartwright, P.; McLean, C.; Sheppard, A.; Rivett, D.; Jones, K.; Dalton, S. LIF/STAT3 controls ES cell self-renewal and pluripotency by a Myc-dependent mechanism. *Development* **2005**, *132*, 885–896. [CrossRef]

Disclaimer/Publisher's Note: The statements, opinions and data contained in all publications are solely those of the individual author(s) and contributor(s) and not of MDPI and/or the editor(s). MDPI and/or the editor(s) disclaim responsibility for any injury to people or property resulting from any ideas, methods, instructions or products referred to in the content.